Hindawi
International Journal of Geophysics
Volume 2023, Article ID 8368175, 14 pages
https://doi.org/10.1155/2023/8368175

Review Article

A Review of Earthquake Source Parameters in the Main Ethiopian Rift

Sisay Alemayehu [1] **and Jima Asefa** [2]

[1] *Institute of Geophysics, Space Science and Astronomy, Addis Ababa University, Box 1176, Addis Ababa, Ethiopia*
[2] *School of Applied Natural Sciences, Department of Applied Physics, Adama Science and Technology University, Box 1888, Adama, Ethiopia*

Correspondence should be addressed to Jima Asefa; ajimaasefa@yahoo.com

Received 14 March 2023; Revised 15 April 2023; Accepted 26 April 2023; Published 11 May 2023

Academic Editor: Angelo De Santis

We assessed earthquake source parameters compiled from previous studies and international databases. In addition, moment tensor inversion is made from the broadband seismic data of two earthquakes that occurred in the region in 2017 and 2018 with magnitudes Mw 5.0 and 5.1, respectively. As a result, the two events' reliable source parameters are retrieved. We found that earthquakes are distributed in the rift floor, at margins and adjacent plateaus. Because the majority of earthquakes occur on the rift floor, deformation is most likely caused by strain accumulation transferred from border faults to magmatic segments along the rift floor. Predominantly normal faulting is observed, but some strike-slip events are also observed. Normal faulting mechanisms are consistent with major plate divergence, whereas the strike-slip components observed in the region might be associated with the counterclockwise rotation of the Danakil microplate, and the mechanism would indicate an oblique-slip deformation between the Nubian plate and the Danakil microplate. However, the focal mechanism obtained from the moment tensor inversion for the Mw 5.1 event indicates dominant normal faulting accompanied by a minor strike-slip component at the western margin of Afar, whereas the Mw 5.0 event has a significant strike-slip component at the central part of MER. The majority of focal depths of earthquakes are found within the upper crust, including the 2017 (Mw 5.0) event with a focal depth of 9.7 km that was computed using moment tensor inversion. A significant number of earthquakes are also found within the lower crust, including the 2018 (Mw 5.1) event with a focal depth of 20.2 km. However, earthquakes with focal depths within the upper mantle are also found in the compiled international database, which may not be consistent with the previously published works in the region. The observed focal depth may suggest a widespread deformation throughout the upper and lower crusts, implying that magmatic intrusions and faulting play a central role in facilitating the seismicity of the main Ethiopian rift (MER). The current investigation will provide further information on the earthquake source parameters and seismogenic depth of earthquake occurrence in the MER.

1. Introduction

The main Ethiopian rift (MER) is one of the most volcanically and seismically active regions in the East African Rift System (EARS). The region has different complex tectonic deformations located at the rift margins and floor (Figure 1). Structurally, the MER marks the two oceanic rifts: the Red Sea and the Gulf of Aden, which are propagating towards a triple-triple-triple junction in the Afar depression [1–4]. The Afar depression is supposed to be linked with the MER at a triple junction [5], where earthquakes are highly distributed (Figure 1), and complex geodynamic deformations reveal several rift structures. Within the MER, the localized magmatism may be extensional through dyking and intrusions [6, 7].

Focal mechanisms of earthquakes may describe a type of deformation and tectonic style. Thus, a clear tectonic style of the MER may provide basic information for defining

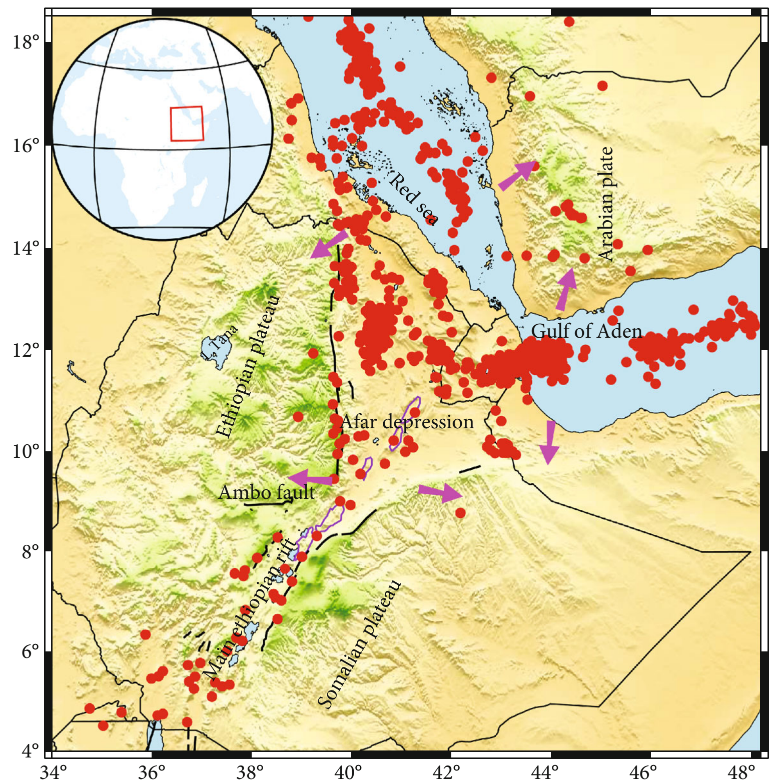

Figure 1: Earthquake distribution and tectonic settings of the MER and the Afar depression. The three major rifts (the Red Sea, the Gulf of Aden, and the main Ethiopian rift) are shown. The red dots are epicentral earthquakes compiled from the United States Geological Survey (USGS) catalog from 1960 to 2019. The magenta arrows show the movements of major plates (Arabian plate and Ethiopian and Somalian plateaus).

kinematics and the detailed faults of the region. In this study, we collect earthquake source parameters computed using first-motion polarities and waveform inversion techniques to assess the seismic activity of the region. We have also computed the source parameters of two earthquakes using a time domain moment tensor inversion from waveform data. The solutions of worldwide earthquake source parameters are available from the Global Centroid Moment Tensor (CMT) catalog [8] and the United States Geological Survey (USGS) catalog, but solutions are available only for strong and moderate earthquakes at different time periods and magnitude thresholds. So far, the kinematics of the study region is mainly based on the focal mechanism of moderate earthquakes computed using first motions down to a lower threshold. Thus, we used source parameters of earthquakes of the MER and surrounding areas to improve the current tectonic knowledge concerning the geodynamic context.

The structurally damaging earthquake, like the Kara Kore earthquake with magnitude 6.4, destroyed the Majete town and was felt within the region [9]. From time to time, significant intermediate earthquakes repeatedly strike several sites in the region. Therefore, good knowledge about the MER current geodynamics is crucial. Recently, earthquakes due to tectonic and volcanic eruptions have attracted human beings. Earthquakes within the MER are historically documented by [9–17] at different times. However, seismic stations used for recording earthquakes in the region are not enough as needed in the past few years [14, 16]. Thus, earthquake source parameters were not properly compiled together, and the detailed study of earthquakes was mostly performed at the local level but poor at the regional level, which needs further investigation. Earthquake source parameters may provide information about the focal mechanisms of earthquakes used to determine fault parameters, and focal depths may give information about the source. Therefore, the current study is aimed at compiling earthquake source parameters that are computed using different techniques and at evaluating the current deformation and the role of magmatic intrusions and faulting in facilitating the seismicity of the MER.

2. Tectonic Setting

The MER is a key rift sector that connects the Red Sea and the Gulf of Aden in the Afar depression, where rifting follows the divergent boundaries of the Nubian, Somalian, and Arabian plates at different tectonic evolution stages [4, 5, 18, 19] (Figure 1). It marks the transition region from continental rifting to incipient seafloor spreading in the Afar depression. The MER is oblique to the end of the southern Red Sea and the Gulf of Aden [20]. Mostly, the MER forms the active plate boundaries of the Nubian and Somalian plates that run through

Ethiopia and significantly influence the orientation and extension of faults [21, 22]. The age from rift initiation to oceanic spreading marks the incipient boundaries between plates through magmatic and tectonic activities [23]. Global and plate tectonic models approximated the rift spreading rate to 5 ± 1 mm/yr and 6 ± 1.5 mm/yr, respectively [24, 25].

The tectonic and dyke intrusions play a central role in facilitating the seismicity within the region [26–29]. In the MER, deformation is focused along 20 km wide, 60 km long magmatic segments [23]. However, strain accumulation is transferred from border faults to the magmatic segments along the rift floor [30]. Thus, an extension has migrated away from the bounding border faults and has localized to rift-aligned magmatic segments at the rift floor [5]. The extension is accommodated through dyking and magmatic underplaying processes for crustal thinning within the region [7].

Crustal thickness beneath the northern and southern parts of the MER and the surrounding areas is not uniformly distributed. The seismogenic thickness might be correlated with the depth of the earthquakes. The elastic and seismogenic thicknesses increase within the MER from northward to southward [31]. For example, crustal thickness increases from 24 km to 38 km as we go from the southern Afar depression to the southern MER [32, 33]. Small- to moderate-magnitude earthquakes may occur at shallow depths in the different parts of the region. Accordingly, earthquakes with focal depths of 5–12 km have been reported in the MER and southern Afar [12, 14, 34]. However, within the region, focal depths down to the lower crust have also been reported.

3. Data and Method

In this work, we compiled focal depths and mechanisms of earthquakes from several published studies [11, 14, 15, 17, 35]. In addition, we used the International Seismological Centre (ISC) and United States Geological Survey (USGS) catalogs. Earthquake source parameters are shown in Table 1 while epicentral earthquake distribution compiled from the USGS catalog is shown in Figure 1. For the compiled results, many controversial solutions for earthquake focal depths are often the case.

We compiled the source parameters of two events from [11]. The source parameters of the six earthquakes that were computed from the moment tensor inversion for the August 2002 earthquake sequence in northern Afar and of the four events that were computed using waveform inversion in a time domain linear inversion algorithm [36, 37] by [14] have been compiled. The source parameters of the seven events that were computed using the full moment tensor inversion using the grid search algorithm of [38, 39] using the 1-D velocity model of [16] have been compiled from [35].

Furthermore, we have compiled the source parameters of earthquakes from several published works that were computed using first-motion polarities. Accordingly, 33 events were compiled from [15] in the northern Ethiopian rift. Focal mechanisms of the events were computed from P and SH wave polarities using the grid search algorithm FOCMEC [40]. In the central MER, 21 events were compiled from [14]. Focal mechanisms of earthquakes were computed using first-motion polarities and amplitude ratios of FOCMEC [40]. In addition, epicentral locations of 4951 events were compiled from [35] (supporting material) as shown in Figure 2. Furthermore, we have compiled earthquake source parameters for larger magnitude earthquakes from the ISC catalog (Table 1), and the epicentral locations of earthquakes compiled from the USGS catalog for the period 1960 to 2019 are plotted in Figure 1.

In addition, three-component broadband waveform data are obtained from the Data Management Center of the Incorporated Research Institutions for Seismology (IRIS DMC) and used for moment tensor inversion. We used broadband data from a minimum of nine phases of seismic stations at epicentral distances in the range of 142–1275 km, successfully recording the 2017 and 2018 earthquakes with magnitudes Mw 5.0 and 5.1, respectively. We selected broadband seismic stations with a high signal-to-noise ratio, and all three-component broadband waveform data qualities were used.

In this study, we applied the moment tensor inversion that efficiently reduces the nonuniqueness of the polarity solutions and better characterizes the earthquake source parameters [41]. Here, we have critically examined the source parameters of two moderate earthquakes using the time domain moment tensor inversion. We used regional broadband data and the 1-D local velocity model of [42]. We applied the approach developed by [43]. Synthetic seismograms are generated and fitted with observed seismograms through bandpass filtering in the time domain range of 0.02–0.05 Hz. Our uncertainty was computed using an error misfit of the L2 norm, which is equal to $\mathrm{sqrt}((d-s)**2)$, where d is the data and s is the synthetics. The L2 norm method is used to minimize the difference between the observed and synthetic seismograms. The best solutions are accepted with errors misfits of 0.521 and 0.497 (L2 norm misfit sense) for earthquakes with Mw 5.0 and 5.1, respectively. Accordingly, the corresponding source parameters are extracted and computed. Here, we used earthquake data from three-component broadband seismic stations, and the selected broadband waveform data are suitable for filtering in a wide range of frequency bands. Several authors have attempted moment tensor inversion from a single-station data, which is even sufficient to generate an accurate solution. However, we used a number of seismic stations and the quality of data in the inversion, which yielded good results [41, 44, 45]. Therefore, we are confident that the solution obtained in this study for source parameters of the event is robustly determined, and we take results as references for the source parameters of earthquakes compiled from different studies and catalogs; thus, the detailed study of earthquakes has been undertaken.

4. Results and Discussion

In this section, the earthquake source parameters compiled from several published works and international databases

Table 1: Source parameters of earthquakes compiled from previously published works and the ISC catalog across the MER. The fault plane solutions are shown in Figures 2(a), 6, and 7, and the final column refers to the work in which the results are published: FJ98 [11], Ay6 [14], Ay7 [14], IK18 [35], and ISC catalog.

Date	Origin time	Longitude (°)	Latitude (°)	Strike (°)	Dip (°)	Rake (°)	Depth (km)	Magnitude	Reference
1987/09/28		36.76	5.79	189	41	-90	9	5.6	FJ98
1987/09/25		36.83	5.49	57	57	127	14	5.6	FJ98
200/05/10	08 : 43 : 28.2	41.08	9.89	126; 288	71; 20	-84; -107	7	4.4	Ay6
2000/05/10	23 : 17 : 52.90	41.08	9.94	86; 310	33; 65	-111; -51	5	4.3	Ay6
2000/05/12	17 : 54 : 02.1	41.04	9.93	91; 290	45; 46	-104; -76	7	4.2	Ay6
200/05/16	20 : 47 : 48.6	41.05	9.91	103; 257	59; 33	-76; -112	6	4.2	Ay6
2002/08/08	21 : 17 : 08.36	39.9798	13.5061	312; 146	56; 44	-260; -79	5	5.0	Ay7
2002/08/10	12 : 01 : 18.68	40.0653	13.865	361; 196	39; 51	258; -80	6	4.4	Ay7
2002/08/10	15 : 55 : 58.41	40.0582	13.5475	322; 172	41; 53	246; -71	7	5.6	Ay7
2002/08/10	16 : 45 : 52.88	40.0193	13.4892	296; 145	55; 39	249; -63	6	4.6	Ay7
2002/08/14	20 : 49 : 22.56	40.1098	13.5665	363; 210	35; 58	247; -74	5	4.5	Ay7
2002/08/25	06 : 02 : 29.12	39.8645	13.4884	317; 143	46; 43	265; -85	6	4.4	Ay7
2007/11/04	21 : 06 : 17	39.9883	13.5427	10.8; 165.2	34.8; 57.9	-68.6; -104.3	10	3.26	IK18
2007/06/11	23 : 44 : 06	39.9697	13.542	165.8; 330.8	38.9; 52.1	-78.2; -99.4	10	2.71	IK18
2008/05/19	17 : 42 : 52	40.169	9.3733	178.8; 65.4	36.1; 73.9	-151.9; -57.3	3	3.57	IK18
2008/05/20	02 : 06 : 00	40.1503	9.3802	67.8; 202.8	34.3; 64.2	-50.4; -113.5	6	4.52	IK18
2008/05/20	02 : 59 : 34	40.0918	9.3188	49.6; 205.7	27.2; 64.9	-68.4;-100.7	4	3.84	IK18
2008/05/26	23 : 32 : 32	40.0098	9.209	82; 192.7	34.9; 76.2	-24.7; -22.3	8	3.76	IK18
2008/05/28	06 : 34 : 49	40.0347	9.2547	76.4; 200.2	31.9; 70.9	-38.3; -16.1	7	4.15	IK18
1999/01/05	18 : 27 : 41.53	37.5589	5.7931	66; 229	47; 44	-78; -102	10	4.6	ISC
1999/06/17	12 : 34 : 55.94	41.3562	10.669	205; 345	30; 66	-54; -109	10	4.4	ISC
2000/07/11		42.228	8.9081	98; 270	43; 47	-84; -97	10	4.7	ISC
2000/05/15	08 : 33 : 03.21	36.229	5.5711	23; 259	49; 58	-134; -51	10	4.9	ISC
2000/05/16	20 : 47 : 53.79	41.062	10.2283	113; 241	60; 43	-57; -133	10	4.4	ISC
2005/09/28	16 : 31 : 38.09	40.687	12.4089	141; 341	55; 36	-102; -74	12	5.1	ISC
2005/09/24	15 : 15 : 34.11	40.4867	12.6171	170; 335	44; 47	-80; -100	12	5.2	ISC
2010/10/02	23 : 24 : 41.94	40.612	11.957	152; 342	50; 41	-97; -82	10	4.9	ISC
2006/04/10	13 : 36 : 48.7	40.26	14.87	172; 335	29; 62	-75; -98	19.9	4.9	ISC
2006/12/21	09 : 07 : 46.95	43.6924	12.0314	133; 270	59; 40	-64; -126	14.7	5.0	ISC
2007/10/20	09 : 06 : 31.00	40.9369	13.3497	10; 110	65; 71	-21; -153	10	5.0	ISC
2008/04/29	00 : 06 : 59.8	42.00	11.7204	96; 300	50; 43	-106; -72	12	5.0	ISC
2009/12/22	03 : 39 : 08.58	40.7081	10.338	22; 146	65; 39	-58; -139	18.7	5.0	ISC
2010/11/14	06 : 32 : 27.14	44.0303	11.9199	90; 299	54; 40	-108; -68	12	5.5	ISC
2007/02/26	08 : 48 : 57.4	43.19	9.77	73; 266	58; 32	-97; -79	12	5.0	ISC
2010/10/23	11 : 08 : 24.8	36.08	4.82	23; 203	55; 35	-90; -90	21	5.0	ISC
2011/03/19	20 : 08 : 10	38.62	6.81	17; 223	51; 42	-108; -70	12	5.0	ISC
2011/06/17	09 : 16 : 12.57	41.76	13.46	10; 101	79; 88	-2; -169	12	5.6	ISC
2011/12/03	02 : 14 : 42.3	36.73	4.75	5; 242	51; 56	-134; -50	12	5.1	ISC
2013/09/18	09 : 04 : 23.66	39.3635	15.8229	31; 130	63; 74	-18; 1-51	22.6	5.1	ISC
2017/01/27	27 : 09 : 24	38.0	7.61	3; 191	45; 45	-96; -84	12	5.3	ISC
2018/03/24	07 : 31 : 20	39.9	13.51	19; 173	56; 37	-75; -111	12	5.2	ISC

are briefly reviewed and related to the pertinent features of the MER. The epicentral locations are plotted in Figures 1 and 2(a), and the focal mechanisms of some events are shown in Table 1. The moment tensor inversion results computed in this study are also shown in Table 2. Accordingly, the magnitudes and focal depths of the two events are Mw 5.0 and 5.1 and 9.7 and 20.2 km for the 2017 and 2018 earthquakes, respectively. Our discussion is based on earthquake distribution, focal depth, and focal mechanism by comparing results obtained from different sources.

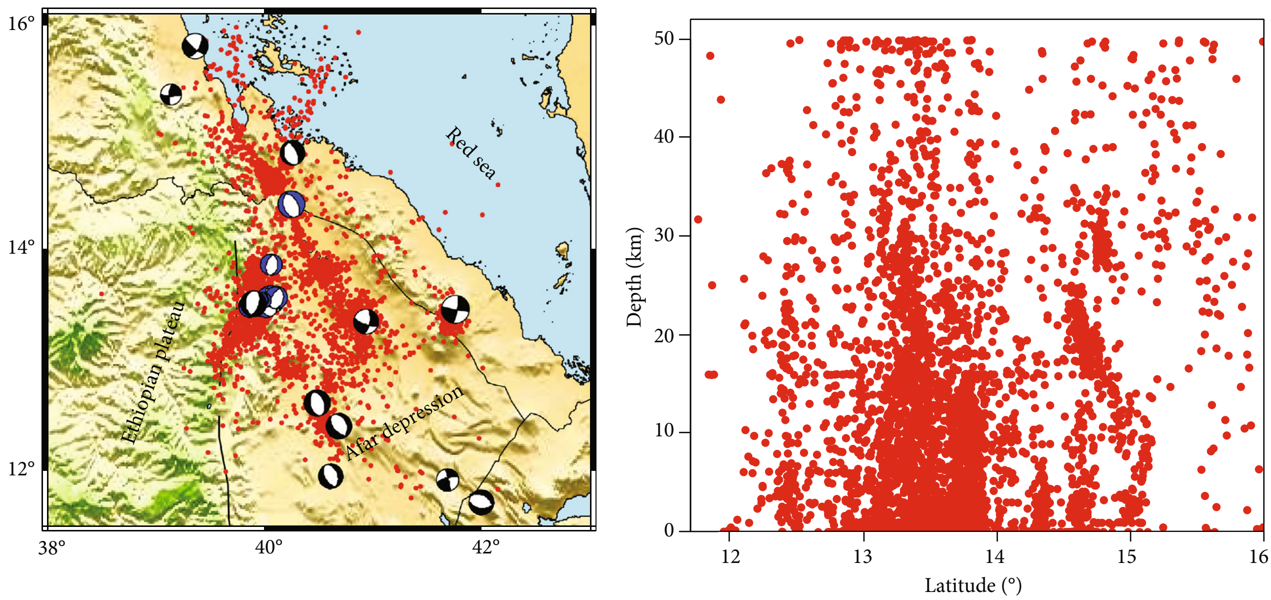

(a) (b)

Figure 2: Epicentral location of earthquakes compiled from the supporting information of [35]: (a) the spatial distribution of earthquakes plotted in this study. Black beach balls represent focal mechanisms compiled from the ISC, and blue beach balls represent the waveform inversions of [14, 35]. (b) The plot of depth vs. latitude of earthquakes from [35].

Table 2: Source parameters of earthquakes computed using moment tensor inversion in this study.

Date	Origin time	Longitude (°)	Latitude (°)	Strike (°)	Dip (°)	Rake (°)	Depth (km)	Magnitude (Mw)
2017/01/27	16:29:23	38.79	7.61	148	85	-152	9.7	5.0
2018/03/24	10:27:31	39.9	13.51	167	24	-124	20.2	5.1

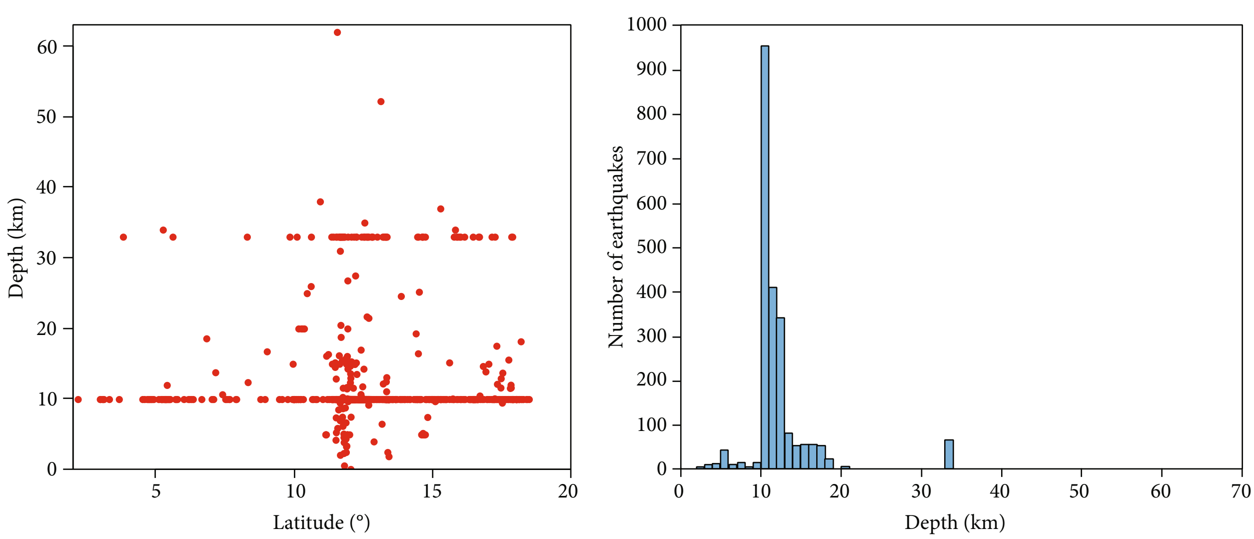

(a) (b)

Figure 3: Spatial distribution of earthquakes: (a) hypocentral depth vs. latitude and (b) histogram of events compiled from the USGS catalog for the period 1960 to 2019.

4.1. Earthquake Distribution. The earthquake distribution is mainly concentrated at the rift floor and rift margins, and very few earthquakes are at adjacent plateaus (see Figures 1 and 2(a)). The Afar depression, the Red Sea, and the Gulf of Aden are very active (Figure 1). In the Afar depression, the trend of earthquake distribution shows the east-west

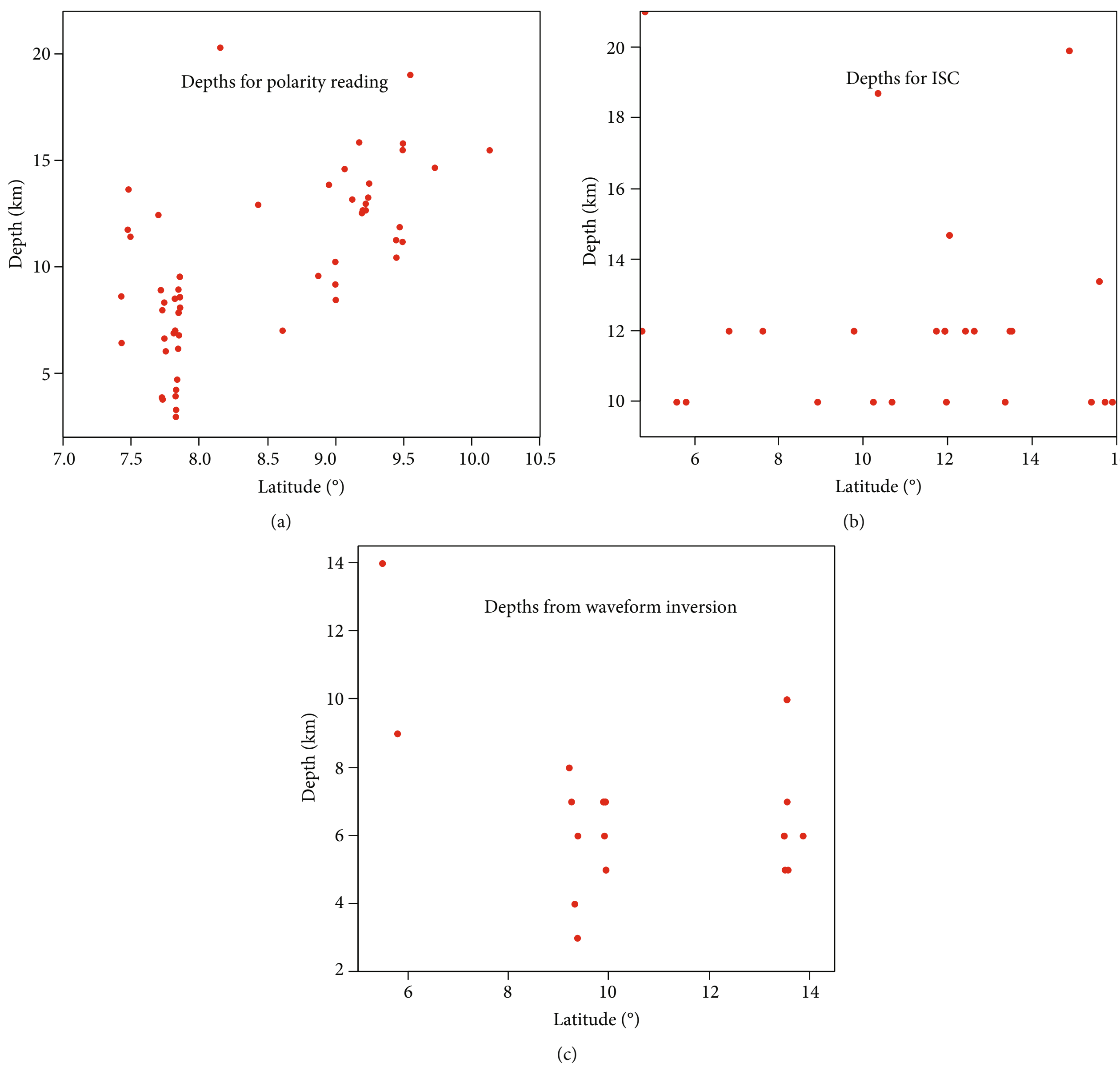

FIGURE 4: Focal depth vs. latitude for earthquakes compiled from different sources as shown in Table 1. (a) Based on the first polarity readings of [15, 17], (b) from the ISC catalog, and (c) from waveform modeling by [11, 14, 35].

elongation of the Gulf of Aden and the NW-SE and NNW-SSE elongations of the Red Sea towards the Afar triple junction (Figure 1). The earthquake distribution is highly concentrated at the rift floor of the Afar depression with sparsely distributed events in the MER (Figure 1). Outside of the rift floor, earthquakes are highly concentrated at the margins of the Afar depression and the northern Ethiopian plateau (Figures 1 and 2(a)). The N-S trending border faults could induce the earthquake distribution near the rift margins of the Ethiopian plateau and might be related to the opening of the Red Sea [5].

We observed that the majority of earthquakes are concentrated along 20 km wide, 60 km long magmatic segments of the rift floor. This indicates that strain accumulation is transferred from border faults to the magmatic segments along the rift floor, and an extension has migrated away from border faults and is localized to rift-aligned magmatic segments at the rift floor. We can conclude that deformation is most likely due to strain accumulation transferred from border faults to the magmatic segments along the rift floor through dyking and magmatism which is underplaying processes for crustal thinning within the region.

The elongations of earthquake clusters generally show a NE-SW trend in the MER, E-W in the Gulf of Aden, and NW-SE in northern Afar (Figure 1). The concentrated seismic activity at the margins of the Ethiopian plateau might have resulted from a high-stress concentration due to the lateral density contrast and differences in lithospheric thickness between the uplifted Ethiopian plateau and the Afar

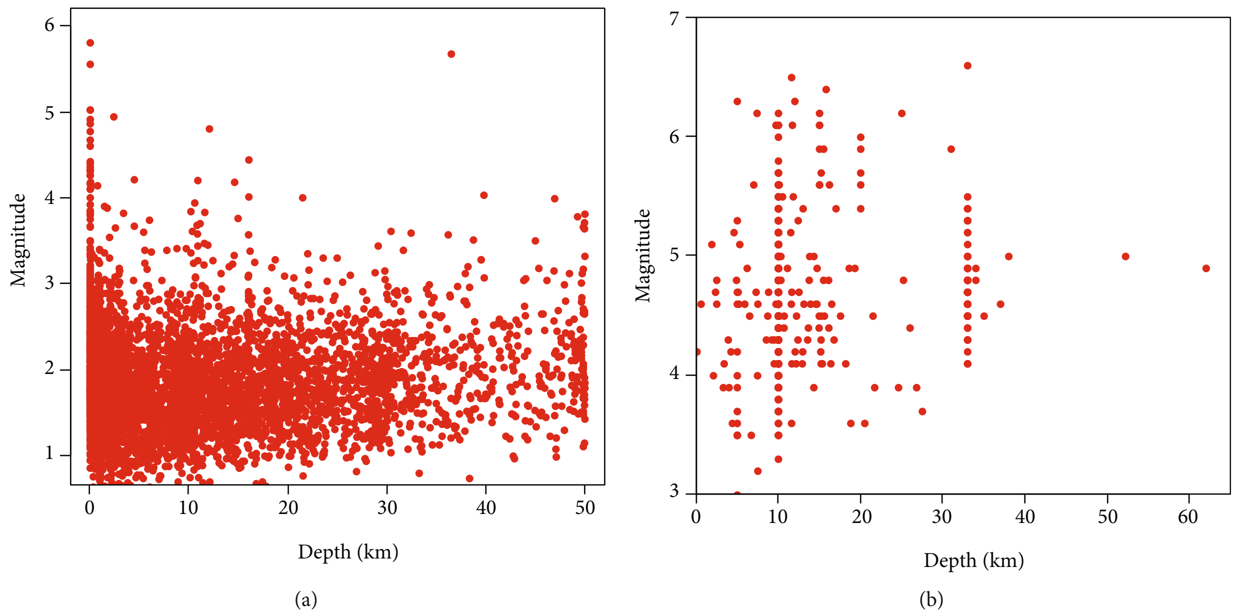

Figure 5: Magnitude of earthquakes versus depth for (a) earthquakes compiled from the supporting information of [35] and (b) earthquakes compiled from the USGS catalog for the period 1960 to 2019.

depression [32, 46]. The margin of the southeastern Ethiopian plateau is seismically not active except for small cluster earthquakes at the southern margin of the Gulf of Aden (see Figure 1). The margin of the central MER is also characterized by scattered earthquakes.

4.2. Hypocentral Distribution. The source parameters of intermediate magnitude earthquakes are determined from waveform modeling, while the first polarity reading is used for small-magnitude earthquakes in several studies in the MER. The plots of the spatial distribution for focal depths are shown in Figures 2(b), 3, and 4, while the plot of the magnitude versus focal depth is shown in Figure 5. The plots for fault plane solutions are shown in Figures 6 and 7.

In our discussion, we compare the hypocentral depths compiled from different sources shown in Figures 2(b), 3, and 4. The largest focal depth of ~50 km is observed, while most earthquakes have shallow depths within 0–30 km (Figure 2(b)). Hypocentral depth distribution has been plotted in Figure 3 for earthquakes compiled from the USGS catalog from 1960 to 2019. Accordingly, the largest focal depth of ~65 km has been observed, but few earthquakes are observed in the range of ~40–65 km. Generally, hypocentral depths range from the near surface to 35 km, and most of earthquakes clustered appear to be fixed at 10 km and 33 km (see the histogram of Figure 3(b)).

On the other hand, earthquake focal depths combined from different previous studies and ISC are shown in Table 1 and Figure 4. Focal mechanisms computed using the first polarity reading have a peak focal depth of ~20 km, while the majority of the earthquakes have focal depths between 3 and 14 km. Events are concentrated within 7°-10°N (Figure 4(a)). The hypocentral depth peak of ~23 km is observed for earthquakes compiled from the ISC catalog, but the majority of earthquakes have focal depths of 10 to 12 km and are concentrated between 4° and 16°N (Figure 4(b)). Furthermore, the source parameters of events that are computed using moment tensor inversion have focal depths of 3–10 km (Figure 4(c)), which is consistent with a brittle-ductile transition zone in the region [14, 31, 42].

Earthquakes compiled from the supporting information of [35] and the USGS catalog for the period 1960 to 2019 have focal depths from the near surface to ~35 km (Figures 2(b) and 3(a)). In general, most events are within the upper crust, which might be due to the stress from nearby faults and dike intrusion in the brittle seismogenic zone of the region at shallow depths. The crust thickness thins dramatically from ~26 to 20 km in Afar [47], whereas it is ~15 km beneath the Danakil depression, suggesting ongoing crustal thinning and magma intrusion [46–48] at shallow depths beneath the region. Thus, relatively deeper earthquakes beneath the region with a focal depth of ~35 km and above may suggest upper mantle earthquakes (Figures 2(b) and 3(a)). However, focal depths of earthquakes as deep as in the upper mantle reported in the compiled international database are not consistent with previously published works in the region which may be due to routine processing problems in the international databases.

Generally, focal depths of different studies show uncommon agreement with each other, and routine processing problems in the international databases should be investigated. Furthermore, the discussion confirmed tectonic and dike intrusions in the brittle seismogenic zone of the region due to ongoing crustal thinning and magma intrusion. There is certainly a problem of large uncertainty in depths reported in international catalogs, especially in the early period.

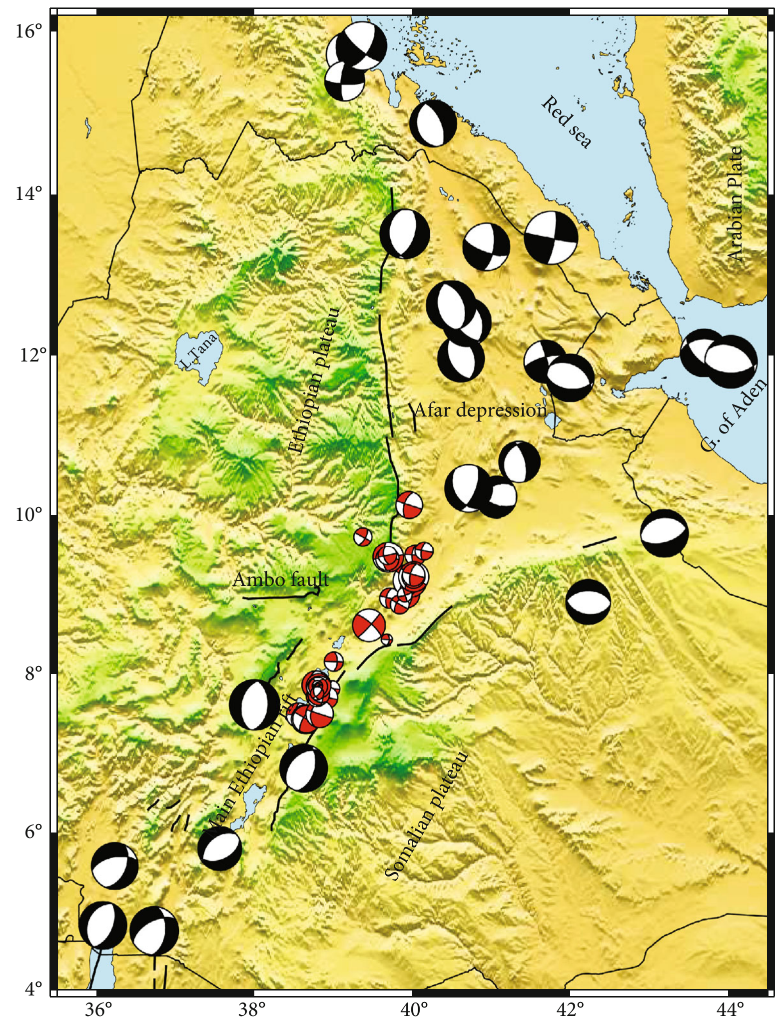

Figure 6: Fault plane solutions of earthquakes in the MER and Afar. Red beach balls represent earthquakes computed from polarity readings from [15, 17], and black beach balls represent earthquakes compiled from the ISC catalog.

Larger earthquake magnitude values of 3.5 to 6.0 (Figure 5(a)) and of 5.5 to 6.5 (Figure 5(b)) are observed with focal depths of 0 to 20 km. The results may suggest and illustrate that relatively larger earthquakes are found to be within the upper crust of the elastic lithospheric thickness of the region.

4.3. Earthquake Focal Mechanism and Its Implications. The fault plane solutions are combined from [11, 14, 15, 17, 35] (ISC) which are computed using moment tensor inversion and polarity readings. The combined fault plane solutions are listed in Table 1 and Figures 2(a), 6, and 7. The focal mechanisms show the existence of normal faulting along the margins of the Ethiopian and Somalian plateaus (Figures 6 and 7). Within the MER and Afar depression, normal faults and strike-slip components are observed (Figures 6 and 7).

Predominantly normal faulting or normal faulting with small strike-slip components is observed in the region, which is in agreement with the previous works of [11, 13, 15]. Fault plane solutions with dominant normal faults and significant strike-slip have been observed at the northern MER and northern Afar with NE-SW and NW-SE trends, respectively. The strike-slip component is also suggested from the previous works of [49, 50]. Only a normal focal mechanism is found in the southern part of MER with a NNE-SSW trend (Figures 2(a), 6, and 7). The interpretation of the focal mechanism might be related to the trend of the MER and the geological observations [51–53] found within the region. Fault plane solutions of some events found in Afar show E-W, N-S, and NNW-SSE trends with roughly north-south and east-west extensions.

In the Afar and Gulf of Aden and at the margin of the Somalia plateau, fault plane solutions of earthquakes may suggest the separation of Arabia from Africa with a north-south extension that is consistent with many focal mechanisms in the central Afar at the triple junction where Arabian plate is now drifting away from Africa plate (Figures 1, 6, and 7). The southern Afar focal mechanisms may show that the region is at the transition zone between the north-south striking southern Red Sea rift fault and the NE trending MER [54]. The strike-slip components

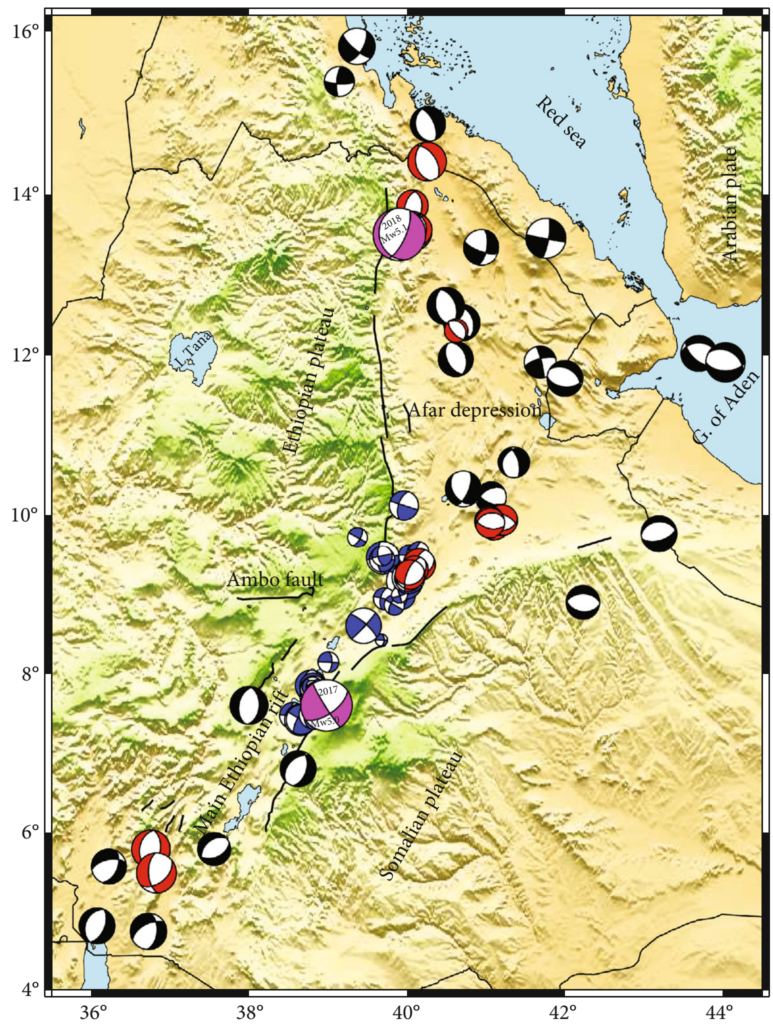

Figure 7: Summary of all fault plane solutions compiled from several regional studies as listed in Tables 1 and 2. The black beach balls represent the focal mechanisms from the ISC catalog, the red beach balls represent the waveform inversion of [11, 14, 15, 35], the blue beach balls represent the polarity reading of [15, 17], and the magenta beach balls represent the focal mechanisms of the 2017 and 2018 earthquakes from which the source parameters are computed using moment tensor inversion from the waveform data. The beach ball size is proportional to the earthquake magnitude, and the solutions show normal faulting with considerable strike-slip components.

observed in the northern Afar might be related to the counterclockwise rotation of the Danakil microplate [25, 55], and the mechanisms would indicate an oblique-slip deformation between the Nubian plate and the Danakil microplate.

The seismically active region of the northern Ethiopian plateau/rift margins (Figures 1 and 2(a)) could have normal focal mechanisms with the NNW-SSW trend (Figures 4 and 6) that could be caused by the north-south trending border faults related to the opening of the Red Sea [5]. Generally, focal mechanisms along the northwestern border of Afar are predominantly showing an east-west extension. The focal mechanism along the eastern border of Afar (the margin of the Somalian plateau) shows an east-west trend with a north-south extension, which might be consistent with the Arabian plateau movement towards the north and the Arabian plateau towards the south, respectively (Figures 6 and 7). Therefore, the north-south extension in the northern part of the region could be related to the Nubian-Arabian plate motion.

Focal mechanisms along the northern and central parts of the MER are mostly normal in style, congruent to the extensional orientation in the rift roughly E-W, while some strike-slip components (Figures 6 and 7) are likely associated with the reactivation of structures found in the region. Only normal faulting with a slightly east-west extension is observed in the southern part of the main Ethiopian rift. The absence of a strike-slip component may suggest that this particular region is neither associated with the microplate rotation (there is no microplate) nor associated with the reactivation of geologic structures.

4.4. Moment Tensor Inversion in the Time Domain. We computed the moment tensor inversion for the 2017 and 2018 earthquakes with magnitudes Mw 5.0 and 5.1, respectively. The moment tensor inversion results are shown in Table 2. Reliable source parameters have been selected for the best fit between observed and synthetic seismograms (Figures 8 and 9). The well-constrained hypocentral depths of the event

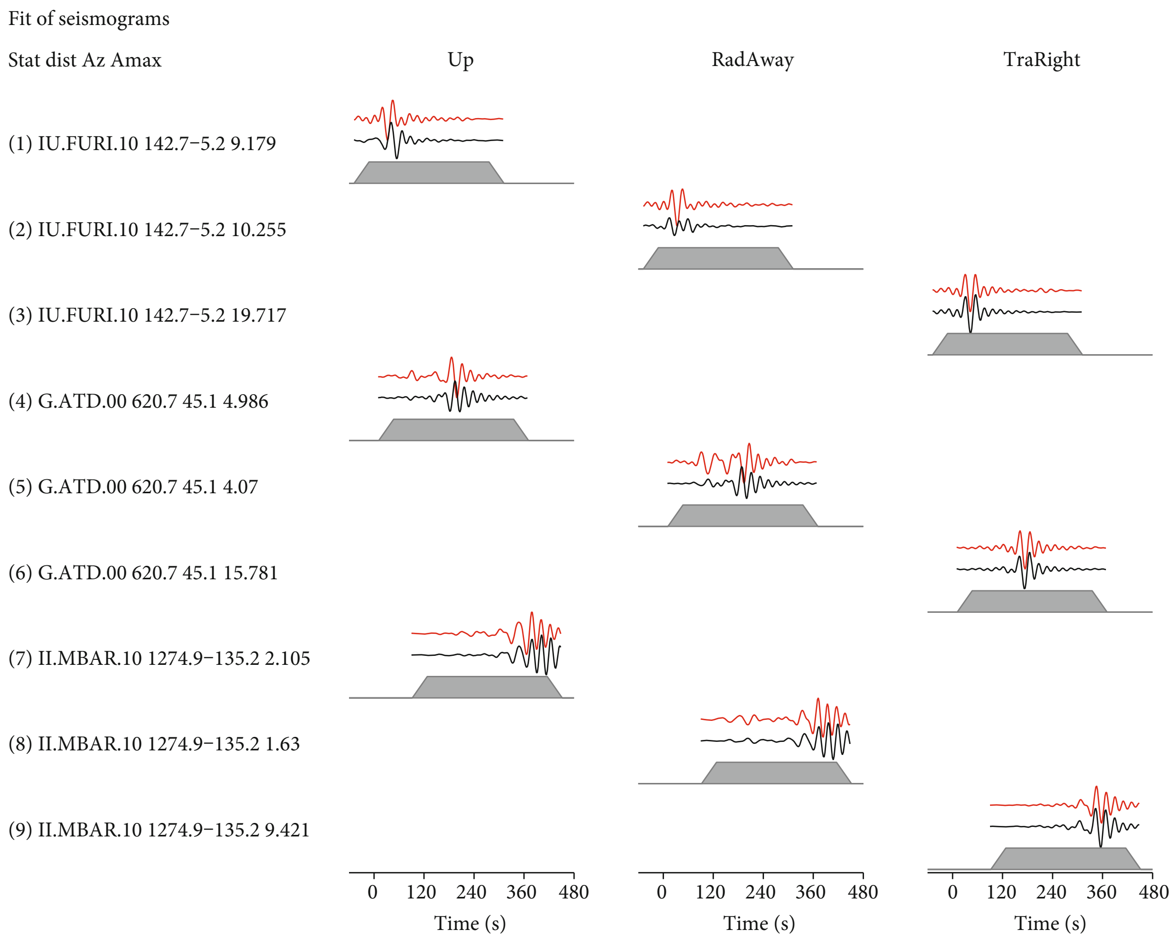

Figure 8: Moment tensor inversion in the time domain for the 2017 earthquake with the magnitude Mw 5.0 that was computed in this study. The panel is dedicated to waveform comparison (red color is used for data and black for synthetics). Stations are sorted based on epicentral distances, with station name, distance, azimuth, and maximal amplitudes on the left side. Up, RadAway, and TraRight of each station are written above the fits of observed and synthetic seismograms.

are estimated to be 9.7 km and 20.2 km for the 2017 and 2018 earthquakes, respectively. The focal depth at 9.7 km is within the upper crust, which might be due to stress from nearby faults and the dike intrusion in the brittle seismogenic zone of the region at a shallow depth beneath the MER, which is consistent with several compiled data. The focal depth at 20.2 km is found near the lower crust within the thinned crust. The lower crust of this particular event might be correlated to a tectonic earthquake that facilitated the deformation of the elastic seismogenic zone of the region due to strain accumulation at the border faults. This indicates the ongoing crustal thinning at the margin of the rift and plateau.

The focal mechanism obtained from the moment tensor inversion for the Mw 5.0 event indicates dominant normal faulting with a significant strike-slip component at the central part of MER (Figure 7). The focal mechanism result indicates two nodal planes oriented along the NW-SE and NE-SW trends. The nodal plane oriented along NW-SE may be chosen as the auxiliary plane, whereas striking along the NE-SW direction is chosen as the fault plane, which might be consistent with the MER trend. Thus, the focal mechanism of this earthquake shows dominantly normal faulting with a significant strike-slip component consistent with the extension of the Ethiopian plateau from the Somalian plateau.

On the other hand, the focal mechanism obtained from the moment tensor inversion for the Mw 5.1 event indicates dominant normal faulting accompanied by a minor strike component at the western margin of Afar. The focal mechanism could have a roughly N-S trending (Figure 7) and could be induced by the north-south trending border faults related to the Red Sea opening [5].

The summary of results from Figures 6 and 7 shows that purely normal faulting and normal faulting with strike-slip components are observed in the MER and Afar depression. The region is dominated by normal faulting due to extensions in the region. On the other hand, the focal mechanism with the strike-slip component observed in the region may suggest the anticlockwise rotation of the Danakil microplate relative to the Nubian plate [25, 55], while some strike-slip components may suggest the reactivation of geologic structures in the region. From our seismicity distribution and focal mechanisms, the Red Sea and Gulf of Aden rifts

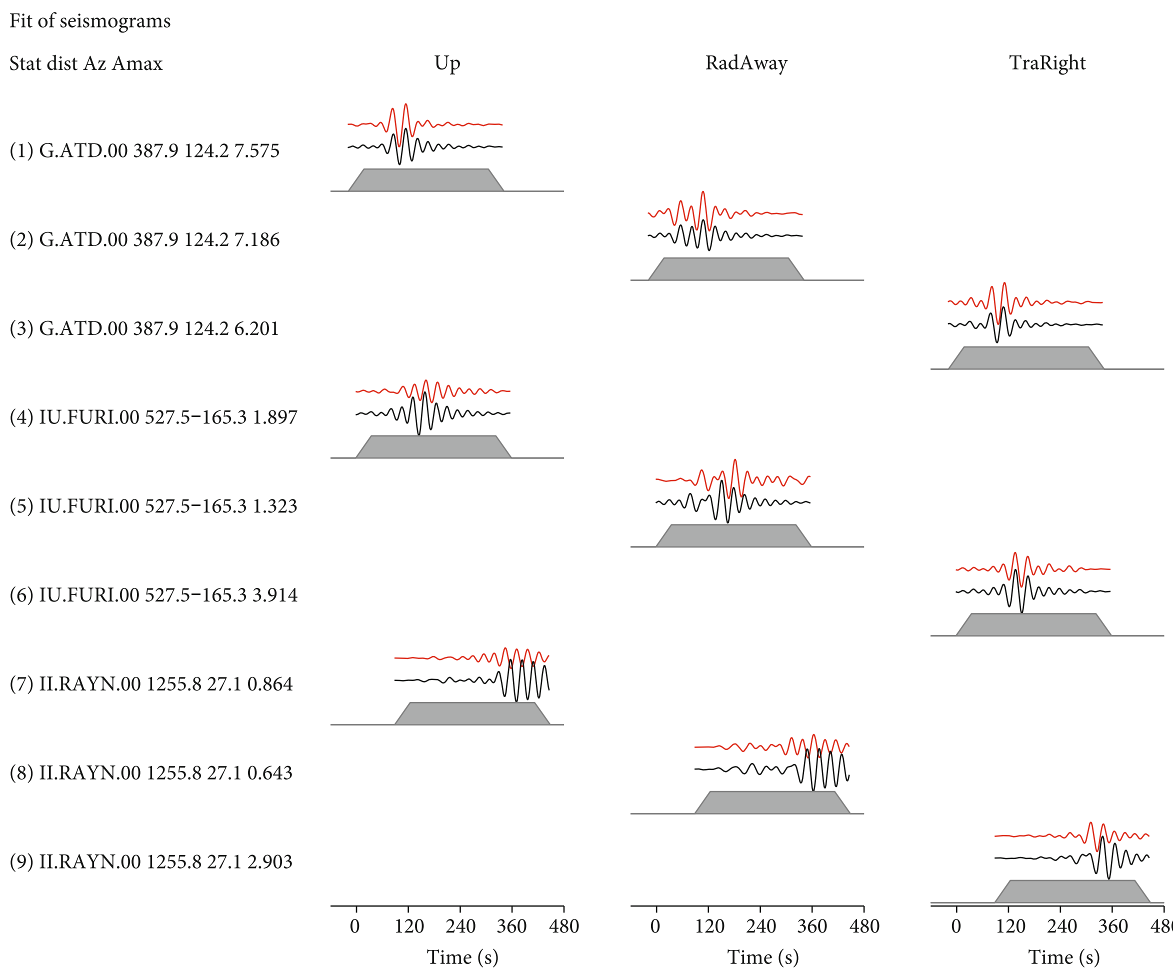

Figure 9: Moment tensor inversion in the time domain for the 2018 earthquake with the magnitude Mw 5.1 that was computed in this study. The panel is dedicated to waveform comparison (red color is used for data and black for synthetics). Stations are sorted based on epicentral distances, with station name, distance, azimuth, and maximal amplitudes on the left side. Up, RadAway, and TraRight of each station are written above the fits of observed and synthetic seismograms.

propagate towards the Afar depression. It is impossible to suggest that the Gulf of Aden is seismically more active than the Red Sea because the two regions are found to be very active (see Figure 1).

From the seismicity distribution and trends of focal mechanisms in the MER and Afar, the geodynamic implications of the region may suggest the separation of the Arabian plate from the African plate in large and the ongoing separation of the Nubian plate from the Somalian plate. In addition, the strike-slip components of the focal mechanism in the region may control the tectonic settings related to the microplate rotation and reactivation of local lineaments. Within the region, earthquakes may be induced by the stress at the rift margins and intrusions in the rift floor. From the hypocentral depth range, deformation throughout the region has been characterized by widespread lithospheric deformations due to inhomogeneous extensions.

5. Conclusions

In this study, we evaluated earthquake source parameters compiled from previous studies and international databases. Furthermore, the moment tensor inversion is performed from broadband seismic data for two earthquakes with magnitudes Mw 5.0 and 5.1 that occurred in the region in 2017 and 2018, respectively. For source parameters of earthquakes compiled from previous studies and obtained from the moment tensor inversion of this study, hypocentral depths of earthquakes are observed in the upper and lower crust ranges. Results from the waveform inversion show that earthquakes are almost from the upper crust, which are consistent with the previous studies. However, hypocentral depths of earthquakes compiled from the international databases are in the range of the crust to the uppermost mantle. The database routine-processing difficulty could result in hypocentral depths reaching the upper mantle. In general, the observed focal depth may suggest broad deformation throughout the upper and lower crusts, implying that magmatic intrusions and faulting are important in promoting seismicity throughout the main Ethiopian rift.

Fault plane solutions revealed normal faulting and strike-slip deformation mechanisms. The northern part of the region is tectonically very complicated, having normal faults with different trends and strike-slip components with different orientations. This implies that the region is undergoing enormous extensions between the three primary plates of the Arabian, Nubian, and Somalian plates, as well as the propagation of the Red Sea, Gulf of Aden, and MER towards the Afar region. Fault plane solutions positioned along the N-S edges of the Ethiopian plateau could be associated with the Red Sea's E-W opening towards the MER. The divergence between the Arabian and Somali plateaus may be revealed through focal mechanisms with E-W trends. The dominantly normal faulting with a significant strike-slip component of the focal mechanism in the central part of MER obtained from the moment tensor inversion has confirmed the extension of the Ethiopian plateau from the Somalian plateau and the striking direction of the MER along the NE-SW. The southern part of the MER fault plane solution indicates the NNE-SSW trend with a roughly E-W extension direction of the rift. The distribution of earthquakes and the trends of focal mechanisms in northern Afar clearly demonstrate the propagation of the Red Sea and the Gulf of Aden towards Afar.

In general, the observed normal faulting mechanisms are consistent with the divergence of the major plates, whereas the observed strike-slip components in the region could be associated with the anticlockwise rotation of the Danakil microplate, and the mechanism would indicate an oblique-slip deformation between the Nubian plate and the Danakil microplate.

Conflicts of Interest

The authors declare that they have no conflicts of interest.

Acknowledgments

We thank the International Seismological Centre (ISC), the United States Geological Survey, and several authors (compiled data from published works) for providing the earthquake data. The International Science Program (ISP) of Uppsala University supports the Ethiopian Seismic Station Network (ESSN).

References

[1] V. Courtillot, "Propagating rifts and continental breakup," *Tectonics*, vol. 1, no. 3, pp. 239–250, 1982.

[2] G. D. Acton, S. Stein, and J. F. Engeln, "Block rotation and continental extension in Afar: a comparison to oceanic microplate systems," *Tectonics*, vol. 10, no. 3, pp. 501–526, 1991.

[3] I. Manighetti, P. Tapponnier, V. Courtillot, S. Gruszow, and P. Y. Gillot, "Propagation of rifting along the Arabia–Somalia plate boundary: the Gulfs of Aden and Tadjoura," *Journal of Geophysical Research*, vol. 102, no. B2, pp. 2681–2710, 1997.

[4] I. Manighetti, P. Tapponnier, P. Gillot et al., "Propagation of rifting along the Arabia–Somalia plate boundary: into Afar," *Journal of Geophysical Research*, vol. 103, no. B3, pp. 4947–4974, 1998.

[5] E. Wolfenden, C. Ebinger, G. Yirgu, A. Deino, and D. Ayalew, "Evolution of the northern Main Ethiopian rift: birth of a triple junction," *Earth and Planetary Science Letters*, vol. 224, no. 1-2, pp. 213–228, 2004.

[6] W. Buck, "Modes of continental lithospheric extension," *Journal of Geophysical Research*, vol. 96, no. B12, pp. 20161–20178, 1991.

[7] G. Mackenzie, H. Thybo, and P. K. H. Maguire, "Crustal velocity structure across the main Ethiopian rift: results from two-dimensional wide-angle seismic modelling," *Geophysical Journal International*, vol. 162, no. 3, pp. 994–1006, 2005.

[8] A. M. Dziewonski, T. A. Chou, and J. H. Woodhouse, "Determination of earthquake source parameters from waveform data for studies of global and regional seismicity," *Journal of Geophysical Research*, vol. 86, no. B4, pp. 2825–2852, 1981.

[9] P. Gouin, *Earthquake history of Ethiopia and the Horn of Africa*, Int. Dev. Res. Centre, Ottawa, Ont, 1979.

[10] A. Ayele and R. Arvidsson, "Fault mechanisms and tectonic implication of the 1985–1987 earthquake sequence in south western Ethiopia," *Journal of Seismology*, vol. 1, pp. 383–394, 1998.

[11] A. N. Foster and J. A. Jackson, "Source parameters of large African earthquakes: implications for crustal rheology and regional kinematics," *Geophysical Journal International*, vol. 134, no. 2, pp. 422–448, 1998.

[12] A. Ayele, "Normal left-oblique fault mechanisms as an indication of sinistral deformation between the Nubia and Somalia plates in the main Ethiopian rift," *Journal of African Earth Sciences*, vol. 31, no. 2, pp. 359–367, 2000.

[13] R. Hofstetter and M. Beyth, "The Afar depression: interpretation of the 1960–2000 earthquakes," *Geophysical Journal International*, vol. 155, no. 2, pp. 715–732, 2003.

[14] A. Ayele, G. Stuart, I. Bastow, and D. Keir, "The august 2002 earthquake sequence in North Afar: insights into the neotectonics of the Danakil microplate," *Journal of African Earth Sciences*, vol. 48, no. 2–3, pp. 70–79, 2007.

[15] D. Keir, C. J. Ebinger, G. W. Stuart, E. Daly, and A. Ayele, "Strain accommodation by magmatism and faulting as rifting proceeds to breakup: seismicity of the northern Ethiopian rift," *Journal of Geophysical Research*, vol. 111, no. B5, article B05314, 2006.

[16] M. Belachew, C. Ebinger, and D. Coté, "Source mechanisms of dike-induced earthquakes in the Dabbahu-Manda Hararo rift segment in Afar, Ethiopia: implications for faulting above dikes," *Geophysical Journal International*, vol. 192, no. 3, pp. 907–917, 2013.

[17] M. Wilks, J. M. Kendall, A. Nowacki et al., "Seismicity associated with magmatism, faulting and hydrothermal circulation at Aluto Volcano, main Ethiopian rift," *Journal of Volcanology and Geothermal Research*, vol. 340, pp. 52–67, 2017.

[18] F. Barberi, S. Borsi, G. Ferarra et al., "Evolution of the Danakil depression (Afar, Ethiopia) in light of radiometric age determinations," *Journal of Geology*, vol. 80, no. 6, pp. 720–729, 1972.

[19] J. R. Cochran, "The Gulf of Aden: structure and evolution of a young ocean basin and continental margin," *Journal of Geophysical Research*, vol. 86, no. b1, pp. 263–287, 1981.

[20] R. Bendick, S. McClusky, R. Bilham, L. Asfaw, and S. Klemperer, "Distributed Nubia-Somalia relative motion and dike intrusion in the main Ethiopian rift," *Geophysical Journal International*, vol. 165, no. 1, pp. 303–310, 2006.

[21] E. Gashawbeza, S. Klemperer, A. Nyblade, K. Walker, and K. Keranen, "Shear-wave splitting in Ethiopia: precambrian mantle anisotropy locally modified by Neogene rifting," *Geophysical Research Letters*, vol. 31, no. 18, 2004.

[22] A. Agostini, M. Bonini, G. Corti, F. Sani, and P. Manetti, "Distribution of quaternary deformation in the Central Main Ethiopian Rift, East Africa," *Tectonics*, vol. 30, no. 4, 2011.

[23] C. Ebinger and M. Casey, "Continental breakup in magmatic provinces: an Ethiopian example," *Geology*, vol. 29, no. 6, pp. 527–530, 2001.

[24] F. P. Jestin, P. Huchon, and J. M. Gaulier, "The Somalia plate and the East African Rift System: present-day kinematics," *Geophysical Journal International*, vol. 116, no. 3, pp. 637–654, 1994.

[25] D. Chu and R. Gordon, "Current plate motions across the Red Sea," *Geophysical Journal International*, vol. 135, no. 2, pp. 313–328, 1998.

[26] R. Pik, B. Marty, and D. Hilton, "How many mantle plumes in Africa? The geochemical point of view," *Chemical Geology*, vol. 226, no. 3-4, pp. 100–114, 2006.

[27] T. Wright, C. Ebinger, J. Biggs et al., "Magma-maintained rift segmentation at continental rupture in the 2005 Afar dyking episode," *Nature*, vol. 442, no. 7100, pp. 291–294, 2006.

[28] K. Keranen, S. Klemperer, J. Julia, J. Lawrence, and A. Nyblade, "Low lower crustal velocity across Ethiopia: is the main Ethiopian rift a narrow rift in a hot craton?," *Geochemistry, Geophysics, Geosystem*, vol. 10, no. 5, 2009.

[29] E. Beutel, J. van Wijk, C. Ebinger, D. Keir, and A. Agostini, "Formation and stability of magmatic segments in the main Ethiopian and Afar rifts," *Earth and Planetary Science Letters*, vol. 293, no. 3-4, pp. 225–235, 2010.

[30] G. Corti, "Control of rift obliquity on the evolution and segmentation of the Main Ethiopian Rift," *Nature Geosciences*, vol. 1, no. 4, pp. 258–262, 2008.

[31] C. Ebinger and N. Hayward, "Soft plates and hot spots: views from Afar," *Journal of Geophysical Research*, vol. 101, no. B10, pp. 21859–21876, 1996.

[32] M. Dugda, A. Nyblade, J. Julia, C. Langston, A. Ammon, and S. Simiyu, "Crustal structure in Ethiopia and Kenya from receiver function analysis: Implications for rift development in eastern Africa," *Journal of Geophysical Research*, vol. 110, no. B1, article B01303, 2005.

[33] P. Maguire, K. Randy, S. Klemper et al., "Crustal structure of the northern main Ethiopian rift from the EAGLE controlled source survey; a snapshot of incipient lithospheric break-up," *Geological Society, London, Special Publications*, vol. 259, no. 1, pp. 269–292, 2006.

[34] L. M. Asfaw, "Development of earthquake-induced fissures in the Main Ethiopian Rift," *Nature*, vol. 297, no. 5865, pp. 393–395, 1982.

[35] F. Illsley-Kepl, D. Keir, J. Bull et al., "Seismicity during continental breakup in the Red Sea rift of northern Afar," *Journal of Geophysical Research: Solid Earth*, vol. 123, no. 3, pp. 2345–2362, 2018.

[36] C. A. Langston, "Source inversion of seismic waveforms: the Koyna, India, earthquakes of 13 September 1967," *Bulletin Seismological Society of America*, vol. 71, no. 1, pp. 1–24, 1981.

[37] C. J. Ammon, R. B. Herrmann, C. A. Langston, and H. Benz, "Faulting parameters of the January 16, 1994 Wyomissing Hills, Pennsylvania earthquakes," *Seismological Research Letters*, vol. 69, no. 3, pp. 261–269, 1998.

[38] D. Dreger, H. Tkalčić, and M. Johnston, "Dilational processes accompanying earthquakes in the Long Valley Caldera," *Science*, vol. 288, no. 5463, pp. 122–125, 2000.

[39] S. Minson and D. Dreger, "Stable inversions for complete moment tensors," *Geophysical Journal International*, vol. 174, no. 2, pp. 585–592, 2008.

[40] J. Snoke, A. Munsey, C. Teague, and A. Bollinger, "A program for focal mechanism determination by combined use of polarity and SV-P amplitude ratio data," *Earthquake Notes*, vol. 55, no. 3, p. 15, 1984.

[41] J. Asefa and A. Ayele, "Complex tectonic deformation in Circum-Tanzania Craton: East African Rift System," *Journal of African Earth Sciences*, vol. 170, article 103893, 2020.

[42] K. Keranen, S. Klemperer, R. Gloaguen, and Eagle Working Group, "Three-dimensional seismic imaging of a protoridge axis in the main Ethiopian rift," *Geology*, vol. 32, no. 11, pp. 949–952, 2004.

[43] S. Cesca, S. Heimann, K. Stammler, and T. Dahm, "Automated procedure for point and kinematic source inversion at regional distances," *Journal of Geophysical Research*, vol. 115, no. B6, pp. 1–24, 2010.

[44] B. Delouis and D. Legrand, "Focal mechanism determination and identification of the fault plane of earthquakes using only one or two near-source seismic recordings," *Bulletin of the Seismological Society of America*, vol. 89, no. 6, pp. 1558–1574, 1999.

[45] J. Zahradník, L. Fojtíková, J. Carvalho, L. Barros, E. Sokos, and J. Janský, "Compromising polarity and waveform constraints in focal-mechanism solutions; the Mara Rosa 2010 Mw 4 central Brazil earthquake revisited," *Journal of South American Earth Sciences*, vol. 63, pp. 323–333, 2015.

[46] C. Tiberi, C. Ebinger, V. Ballu, G. Stuart, and B. Oluma, "Inverse models of gravity data from the Red Sea-Aden-East African rifts triple junction zone," *Geophysical Journal International*, vol. 163, no. 2, pp. 775–787, 2005.

[47] J. Hammond, J. Kendall, G. Stuart et al., "The nature of the crust beneath the Afar triple junction: evidence from receiver functions," *Geochemistry, Geophysics, Geosystems*, vol. 12, no. 12, 2011.

[48] I. Bastow and D. Keir, "The protracted development of the continent-ocean transition in Afar," *Nature Geoscience*, vol. 4, no. 4, pp. 248–250, 2011.

[49] D. Mckenzie, D. Davies, and P. Molnar, "Plate tectonics of the Red Sea and East Africa," *Nature*, vol. 226, no. 5242, pp. 243–248, 1970.

[50] F. Kebede, W. Y. Kim, and O. Kulhánek, "Dynamic source parameters of the March–May 1989 Serdo earthquakes in central Afar, Ethiopia, deduced from teleseismic body waves," *Journal of Geophysical Research*, vol. 170, no. 3-4, 1989.

[51] B. Abebe, M. Boccaletti, R. Mazzuoli, M. Bonini, L. Tortorici, and T. Trua, *Geological map of the Lake Ziway-Asela region (Main Ethiopian Rift), scale 1: 50, 000*, Cons. Naz. delle Ric., A. R. C., A. Florence, Italy., 1998.

[52] M. Casey, C. Ebinger, D. Keir, R. Gloaguen, and F. Mohamed, "Strain accommodation in transitional rifts: extension by magma intrusion and faulting in Ethiopian rift magmatic segments," *Geological Society, London, Special Publications*, G. Yirgu, C. J. Ebinger, and P. K. H. Maguire, Eds., vol. 259, no. 1, pp. 143–163, 2006.

[53] A. Pizzi, M. Coltorti, B. Abebe, L. Disperati, G. Sacchi, and R. Salvini, "The Wonji Fault Belt (main Ethiopian Rift): structural and geomorphological constraints and GPS monitoring," *Geological Society, London, Special Publications*, vol. 259, no. 1, pp. 191–207, 2006.

[54] S. Tesfaye, D. J. Harding, and T. M. Kusky, “Early continental breakup boundary and migration of the Afar triple junction, Ethiopia,” *Geological Society of America Bulletin*, vol. 115, no. 9, p. 1053, 2003.

[55] G. Eagles, R. Gloaguen, and C. Ebinger, “Kinematics of the Danakil microplate,” *Earth and Planetary Science Letters*, vol. 203, no. 2, pp. 607–620, 2002.